

Time-dependent Hartree-Fock calculations of fusion cross sections for $^{16}\text{O} + ^{40}\text{Ca}$ and $^{28}\text{Si} + ^{28}\text{Si}$

P. Bonche

Service de Physique Théorique, CEN Saclay, BP n°2, 91190 Gif-sur-Yvette, France

K. T. R. Davies

Physics Division, Oak Ridge National Laboratory, Oak Ridge, Tennessee 37830

B. Flanders

W. K. Kellogg Radiation Laboratory, California Institute of Technology, Pasadena, California 91125

H. Flocard

Division de Physique Théorique, Institut de Physique Nucléaire, BP n°1, 91406, Orsay, France

B. Grammaticos

Service de Physique Théorique, CRN de Strasbourg, BP n°20, Cro, 67037 Strasbourg, France

S. E. Koonin

W. K. Kellogg Radiation Laboratory, California Institute of Technology, Pasadena, California 91125

S. J. Krieger

Department of Physics, University of Illinois at Chicago Circle, Chicago, Illinois 60680

M. S. Weiss

Lawrence Livermore Laboratory, University of California, Livermore, California 94550

(Received 24 April 1979)

Time-dependent Hartree-Fock calculations are carried out for the systems $^{16}\text{O} + ^{40}\text{Ca}$ and $^{28}\text{Si} + ^{28}\text{Si}$. Cross sections for the formation of ^{56}Ni are qualitatively similar in both cases, although there exist significant quantitative differences which reflect the importance of the entrance channel. Both systems exhibit an angular momentum window for fusion. The results of the calculations are compared with currently available experimental data.

[NUCLEAR REACTIONS $^{16}\text{O}(^{40}\text{Ca}, x)$ and $^{28}\text{Si}(^{28}\text{Si}, x)$ in time-dependent Hartree-Fock approximation. Fusion and strongly damped collisions.]

I. INTRODUCTION

Although the time-dependent Hartree-Fock (TDHF) approximation was formulated¹ 50 years ago, it is the last 3 years in which the approximation has been seriously applied to the calculation of physical quantities in heavy ion collisions. In this brief span, we have witnessed a remarkably rapid evolution from the early one-dimensional calculations,^{2,3} which reproduced the qualitative features of colliding heavy ions, to increasingly more ambitious two-dimensional calculations,⁴⁻¹⁴ and finally to three-dimensional calculations¹²⁻¹⁸ which yield quantitatively accurate descriptions of certain experimental data. In the present work, the TDHF approach is applied to the calculation of fusion cross sections for two systems, $^{16}\text{O} + ^{40}\text{Ca}$ and $^{28}\text{Si} + ^{28}\text{Si}$, both of which lead to the compound nucleus ^{56}Ni . Although the primary purpose of this work is to compare the results of the TDHF

calculations with experimental data, we shall also discuss the accuracy of the two-dimensional rotating frame and separable approximations to the fully three-dimensional TDHF calculations. In addition, we shall discuss the effect of removing the isospin symmetry restriction on the nuclear wave function, and of varying the parameters of the nuclear potential.

II. METHOD OF CALCULATION

Most of the calculations presented here employ the parametrization of the Skyrme potential¹⁹ referred to as Force I in Ref. 18. In this version of the potential, the nonlocal terms in the mean field proportional to the Skyrme parameters t_1 and t_2 are identically zero. At the highest energies, the full Skyrme potential including the nonlocal terms has also been used to calculate the fusion cross section. The effect on the fusion

cross section of varying the Skyrme parameters is also discussed in Ref. 18, and in Ref. 11.

The calculations have been carried out using the two-dimensional separable approximation^{12,14} and the two-dimensional rotating frame approximation^{4,5,13} to the TDHF equations. In addition, in order to verify the accuracy of the separable approximation, the $^{16}\text{O} + ^{40}\text{Ca}$ fusion cross section has also been calculated at selected energies using the fully three-dimensional TDHF code.^{13,17} It should be noted that in effecting this comparison we have employed codes, both the separable code and the three-dimensional code, which enforce isospin symmetry. That is, neutrons and protons which occupy the same orbital are constrained to be degenerate. This degeneracy is not enforced in the rotating frame approximation^{4,5,13} code, and we shall therefore be able to comment upon the effect of lifting the isospin degeneracy. As the various numerical methods which are employed to solve the TDHF equations have been discussed extensively in the references cited, we shall not comment upon them further here.

The fusion cross sections for $^{16}\text{O} + ^{40}\text{Ca}$ and $^{28}\text{Si} + ^{28}\text{Si}$ have been calculated as follows. For each of the energies studied, the maximum value of angular momentum for which fusion takes place, $l_{\text{max}}\hbar$, and the minimum value of angular momentum for which fusion takes place, $l_{\text{min}}\hbar$, are separately determined to a precision of approximately $2\hbar$. The fusion cross section is then calculated at each energy by the sharp cutoff formula¹⁸

$$\sigma_{\text{fusion}} = \frac{\pi}{k^2} \sum_{l=l_{\text{min}}}^{l_{\text{max}}} (2l+1), \quad (2.1)$$

in which k represents the relative wave number in the entrance channel. For the asymmetric system $^{16}\text{O} + ^{40}\text{Ca}$, the sum extends over all partial waves for which fusion occurs. For the symmetric system $^{28}\text{Si} + ^{28}\text{Si}$, the sum in Eq. (2.1) is replaced by twice the sum over all even partial waves for which fusion occurs. The values of l for which fusion does occur are determined at each energy by evolving the system at various impact parameters for a sufficiently long period of time to offer convincing evidence that the system will not undergo prompt fission. A more detailed discussion of the latter point may be found in Ref. 11. Although the sums to which we refer above may easily be evaluated exactly, it is consistent with the nature of the approximation to use, for either symmetric or asymmetric systems, the result

$$\begin{aligned} \sigma_{\text{fusion}} &\simeq \frac{\pi}{k^2} [(l_{\text{max}}+1)^2 - (l_{\text{min}}+1)^2] \\ &= \frac{\pi\hbar^2}{2\mu E_{\text{c.m.}}} [(l_{\text{max}}+1)^2 - (l_{\text{min}}+1)^2], \end{aligned} \quad (2.2)$$

in which μ represents the reduced mass of the system under consideration.

III. RESULTS

A. $^{16}\text{O} + ^{40}\text{Ca}$

We have performed calculations for the $^{16}\text{O} + ^{40}\text{Ca}$ system for laboratory bombarding energies from 40 MeV to 350 MeV. The calculations have been carried out in the two-dimensional separable approximation^{12,14,30} and in the two-dimensional rotating frame approximation.^{4,5,13} In addition, selected points have been calculated using the fully three-dimensional TDHF code.^{13,17} In all cases which have been compared, the separable fusion cross sections have been in complete agreement with the fully three-dimensional TDHF calculations. A graphic demonstration of this agreement is given in Fig. 1, in which the fragment separation coordinate r , defined as in Ref. 5, is plotted as a function of time for a collision at a laboratory energy of 290 MeV, in which the initial angular momentum, l , is equal to 48. The results of the two-dimensional separable approximation are in very good agreement with the results of the fully three-dimensional calculation, until $t \approx 9 \times 10^{-22}$ s, by which time the system has fused. Plots of the

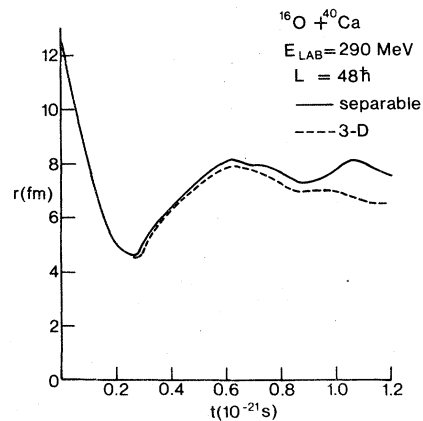


FIG. 1. Comparison, as a function of time, of the fragment separation coordinate in a collision between ^{16}O and ^{40}Ca ions at a laboratory energy of 290 MeV with $l = 48$. The solid line gives the result of the two-dimensional separable approximation, and the dashed line gives the result of the fully three dimensional calculation. In both calculations, the neutron and proton orbitals are degenerate.

quadrupole moments of the mass distribution exhibit similar behavior.

The angular momenta for which the $^{16}\text{O}+^{40}\text{Ca}$ system fuses are depicted as a function of the center of mass energy in Fig. 2. The values plotted are derived from calculations which employ the separable two-dimensional code with degenerate neutron and proton orbitals. The maximum angular momentum which the fused system can sustain is approximately 60 units of \hbar . This value is in good agreement with the prediction $58\hbar$ of the liquid drop model²⁰ for the $A=56$ system. The fact that there exists a minimum angular momentum, $l_c(E)$, for which the $^{16}\text{O}+^{40}\text{Ca}$ system fuses, represents a dramatic prediction of the TDHF calculations.²⁷ Referring again to Fig. 2, we note that as the center of mass energy increases above 100 MeV, l_c likewise increases. This reflects the inability of the colliding ions to convert sufficient translational energy to internal excitation energy. The inability of the transient fused system to dissipate more radial kinetic energy than a certain amount is an essential feature of the mean field dynamics.²¹ The increase of l_c with energy causes the fusion cross section to decrease more rapidly than $1/E_{c.m.}$, which represents the energy dependence of Eq. (2.2) in the absence of l_c , for energies greater than $E_{c.m.} \sim 160$ MeV. At the latter energy, the saturation angular momentum, $l \sim 60$, has been reached, and, in the absence of l_c , the energy dependence is given simply by the kinematical factor $1/E_{c.m.}$. The actual existence of a lower fusion limit could thus be inferred from the decrease with energy of the experimental fusion cross section for energies $E_{c.m.} > 160$ MeV.

The $^{16}\text{O}+^{40}\text{Ca}$ fusion cross section, as given by Eq. (2.2) is compared with the experimental cross section in Fig. 3. The theoretical results pre-

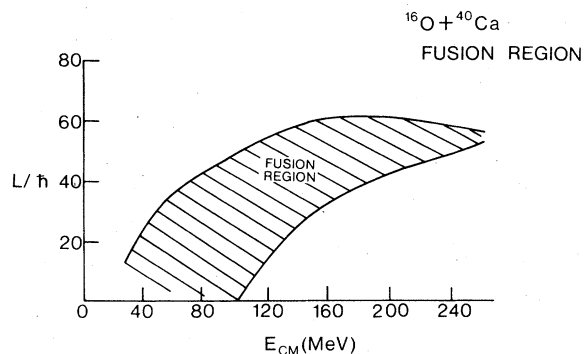


FIG. 2. Fusion region in the angular momentum-energy plane for the system $^{16}\text{O}+^{40}\text{Ca}$. The calculations have been effected with the separable code using the local Skyrme interaction, and with neutron and proton orbitals degenerate.

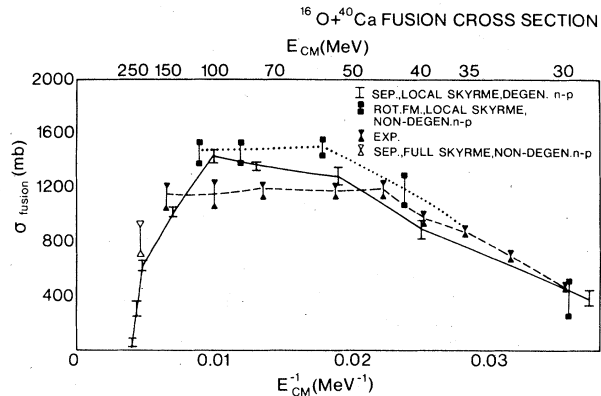


FIG. 3. Comparison of the calculated fusion cross section with the results of experiment (Ref. 24) for $^{16}\text{O}+^{40}\text{Ca}$. Plotted are the results of calculations using the separable code with the local Skyrme interaction and degenerate neutron and proton orbitals, the results of calculations using the rotating frame approximation with the local Skyrme interaction and unrestricted neutron and proton orbitals, and the result of a single calculation at 208 MeV using the separable code with the full Skyrme interaction and unrestricted neutron and proton orbitals.

sented have been calculated using both the results of the two-dimensional, separable approximation with constrained neutron and proton orbitals, and the two-dimensional rotating frame approximation in which no isospin symmetry has been enforced. As we have previously noted, the separable results are in complete agreement with the results of fully three-dimensional TDHF calculations (with the same enforced isospin symmetry). The cross section computed using the results of the rotating frame approximation exceeds the cross section calculated using the results of the separable approximation by approximately 120 mb in the energy range from just above the fusion barrier to $E_{c.m.} \sim 100$ MeV. This difference may be attributed entirely to the enforced neutron-proton degeneracy in the separable calculations. At center of mass energies above 100 MeV, a significant amount of the dissipated energy excites nonaxial modes, and the rotating frame approximation breaks down. Thus, although the upper limit for fusion, $l > 50$, is accurately given by the rotating frame approximation at $E_{c.m.} \sim 100$ MeV, the approximation incorrectly indicates that the system will not fuse at $l=15$. The latter results are qualitatively the same as those found in Ref. 11, in which the lifting of the isospin restriction on the nuclear wave function resulted in an increase of approximately 200 mb in the $^{40}\text{Ca}+^{40}\text{Ca}$ fusion cross section, and the excitation of nonaxial modes caused the rotating frame approximation to break down in the $^{40}\text{Ca}+^{40}\text{Ca}$ system at a center of mass

energy on the order of 100 MeV, the approximate energy at which the angular momentum window appears in the three-dimensional calculations.

Referring to Fig. 3, in which the fusion cross section is plotted as a function of the energy, we note that the theoretical results are in good agreement with the experimental results at low energy. This agreement at low energy affirms the facts that the nuclear sizes and the inter-ion potential are accurately given by the TDHF wave functions and the nucleon-nucleon interaction. However, at energies $E_{c.m.} \approx 100$ MeV, the theoretical cross section exceeds the measured cross section by $\approx 25\%$. In discussing the discrepancy between theory and experiment it should be noted that a significant amount of fusion followed by fission is consistent with the prediction of the liquid drop model²² for the mass 56 system. Moreover, such events would not have been observed in the evaporation residue experiments with which we are making our comparison. However, separate investigations²³ do not indicate that there exists sufficient fusion-fission cross section to account for the discrepancy between the theoretical and experimental results. The fact that the TDHF cross section exceeds the experimental cross section especially warrants further study, since corrections to TDHF would be expected, at least naively, to result in an increased fusion cross section.

We have also performed a single calculation at $E_{c.m.} = 208$ MeV, using the separable approximation with the full Skyrme interaction¹¹ and the isospin symmetry restriction removed. The fusion cross section computed on the basis of this calculation is 823 ± 121 mb. Referring to Fig. 3, we note that the cross section at this energy, as calculated using the results of the separable calculation with the local Skyrme interaction and degenerate neutron and proton orbitals is approximately 600 mb. The difference in cross section of the calculations is thus 220 ± 120 mb. Since approximately 120 mb of this difference can be attributed to the removal of the isospin symmetry restriction, no definitive statement can be made as to the effect of the nonlocal terms in the Skyrme potential.

B. $^{28}\text{Si} + ^{28}\text{Si}$

We have performed calculations for the $^{28}\text{Si} + ^{28}\text{Si}$ system for laboratory bombarding energies from 70 MeV to 220 MeV. The calculations have been carried out in the two-dimensional separable approximation, with the initial, static wave function for the system determined in a filling approximation, in which the occupation of each $1s-0d$ orbital of the separated ^{28}Si ions is set equal to 0.5. In essence, this approximation represents an average

over the possible initial orientations of the deformed Slater determinants of the separated ^{28}Si ions. As such it is a physically reasonable (and computationally necessary) approximation to the actual scattering. It nevertheless represents a departure from, and approximation to, a true TDHF calculation.

The angular momenta for which the $^{28}\text{Si} + ^{28}\text{Si}$ system fuses are depicted as a function of the energy in Fig. 4. The maximum angular momentum which the fused system can sustain can be inferred to be approximately $50\hbar$. Since the fused $^{16}\text{O} + ^{40}\text{Ca}$ system has been calculated to sustain $60\hbar$, it might appear that the maximum angular momentum depends upon the entrance channel, and is not a function only of the total charge and mass of the system, as given by the liquid drop model. This conclusion, however, is considerably obscured by the fact that the $^{28}\text{Si} + ^{28}\text{Si}$ calculation has been effected in the filling approximation. We shall discuss this point more fully at the conclusion of this section. As in the case of the $^{16}\text{O} + ^{40}\text{Ca}$ system, we find a fusion window in the $^{28}\text{Si} + ^{28}\text{Si}$ vs $E_{c.m.}$ plot. For center of mass energies greater than 54 MeV, the $^{28}\text{Si} + ^{28}\text{Si}$ system exhibits no fusion when the angular momentum of the system is less than a cutoff value, $l_c(E)$, which increases as a function of bombarding energy. An unexpected result of the $^{28}\text{Si} + ^{28}\text{Si}$ calculations is the partial closing of the fusion window in the energy range above 100 MeV. This effect is manifest in Fig. 4, in which the fusion region in the angular momentum-energy plane is plotted for the $^{28}\text{Si} + ^{28}\text{Si}$ system. The results of the calculations effected in this energy range have been explicitly plotted.

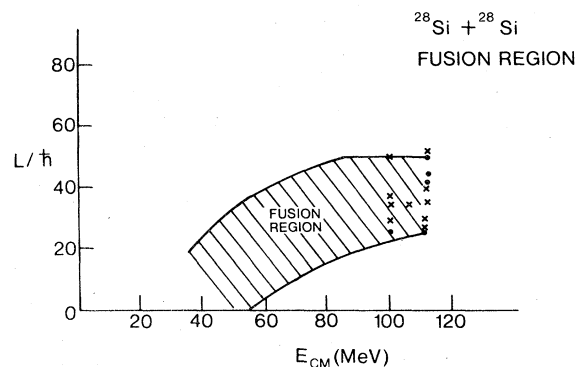


FIG. 4. Fusion region, in the angular momentum-energy plane, for the system $^{28}\text{Si} + ^{28}\text{Si}$. The calculations have been effected with the separable code using the local Skyrme interaction, and with neutron and proton orbitals degenerate. For energies above 100 MeV, the results of the calculations have been explicitly plotted, with crosses used to indicate events in which the ^{28}Si ions scatter, and dots used to indicate events in which the ^{28}Si ions fuse.

Thus, the crosses represent calculations in which the ^{28}Si ions scatter, and the dots represent calculations in which the ^{28}Si ions fuse. An island of nonfusion events is clearly visible in this energy range. While such dramatic variation, associated with only minor changes in the initial conditions did occur in the very first one-dimensional calculations,² it is more probable that the appearance of the island signals a breakdown of the two-dimensional separable approximation. For a fully three-dimensional calculation effected in the center of the island of nonfusion events indeed leads to fusion. It is thus possible that the two-dimensional separable approximation breaks down at high energy, where the fusion cross section goes to zero. Accordingly, we shall assume that the island of nonfusion events is spurious, and shall ignore it in the computation of the fusion cross sections.

The fusion cross section for $^{28}\text{Si} + ^{28}\text{Si}$ is plotted as a function of energy in Fig. 5. The behavior of the cross section is qualitatively similar to that of $^{16}\text{O} + ^{40}\text{Ca}$, although the latter system exhibits a more pronounced plateau at intermediate energies, and drops more precipitously at high energy. A comparison of Fig. 2 and Fig. 4 shows that the faster decrease of the $^{16}\text{O} + ^{40}\text{Ca}$ cross section is due to the more rapid closing of the fusion window of the latter reaction. As the energy increases, l_c increases more rapidly for the $^{16}\text{O} + ^{40}\text{Ca}$ system than for the $^{28}\text{Si} + ^{28}\text{Si}$ system. It should be noted, however, that this high energy comparison may be complicated by the unexpected behavior of the $^{28}\text{Si} + ^{28}\text{Si}$ system at energies above $E_{c.m.} = 100$ MeV, as given by the separable approximation.

In Fig. 6, the center of mass energy loss and scattering angle, as calculated in the separable

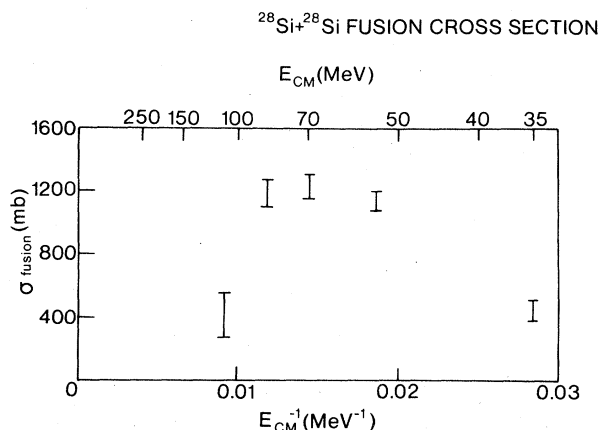


FIG. 5. Calculated fusion cross section for $^{28}\text{Si} + ^{28}\text{Si}$. The calculations have been effected using the code as described in Fig. 4.

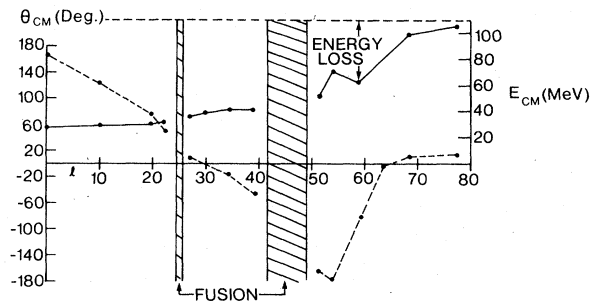


FIG. 6. Deflection and energy loss functions for $^{28}\text{Si} + ^{28}\text{Si}$ at a center of mass energy of 111 MeV. The calculations have been effected using the code as described in Fig. 4.

approximation, are plotted as functions of angular momentum for $^{28}\text{Si} + ^{28}\text{Si}$ at $E_{c.m.} = 111$ MeV. The curves are qualitatively similar to results obtained⁵ for $^{16}\text{O} + ^{16}\text{O}$ and $^{40}\text{Ca} + ^{40}\text{Ca}$. However, an important distinction is the fact that the systems and energies investigated in Ref. 5 did not lead to fusion. As discussed above, the scattering events observed in reactions in which the angular momentum of the system is in the range $27 \leq l \leq 39$ are quite possibly spurious. Fully three-dimensional calculations would likely lead to fusion in this interval.

Although experimental data are not available for the $^{28}\text{Si} + ^{28}\text{Si}$ system, measurements have recently been made²⁵ on the similar $^{32}\text{S} + ^{27}\text{Al}$ system. In their investigation of the latter system at a laboratory energy of 175 MeV, Natowitz *et al.*²⁵ can explain the observed spectrum by assuming the existence of two strongly damped components in the energy spectrum of the reaction products. One component is inferred to correspond to an angular momentum $l \approx 48$, not inconsistent with the liquid drop expectation that the $A = 59$ system will not support angular momentum ≥ 58 . In contrast, the second component is inferred to correspond to very low values of angular momentum, $l \leq 15$. As a result of their analysis, Natowitz *et al.*²⁵ conclude that the observation of scissioning nuclei with such small angular momenta can be explained if the lowest partial waves in the entrance channel lead to strongly damped collisions, rather than to fusion. This situation is precisely that found in the $^{28}\text{Si} + ^{28}\text{Si}$ system. At $E_{c.m.} = 80$ MeV, the same center of mass energy as in the $^{32}\text{S} + ^{27}\text{Al}$ experiment, we find that the $^{28}\text{Si} + ^{28}\text{Si}$ fusion window is open for angular momenta $17 \leq l \leq 48$. Further comparison can be made with the fragment energies for collisions at angular momenta just outside the window. Natowitz *et al.*²⁵ find a center of mass fragment kinetic energy of 16.6 MeV for the $l \approx 15$ component, and a fragment

kinetic energy of 26.4 MeV for the $l \approx 48$ component. TDHF calculations of the $^{28}\text{Si} + ^{28}\text{Si}$ system at $E_{c.m.} = 80$ MeV show that the fragments in collisions with $l = 16$ carry 16 MeV kinetic energy, and fragments in collisions with $l = 49$ carry 28 MeV kinetic energy. The results of the $^{28}\text{Si} + ^{28}\text{Si}$ calculations are thus consistent with this interpretation of the $^{32}\text{S} + ^{27}\text{Al}$ data.

We mentioned above that any conclusion as to the existence of entrance channel effects is significantly obscured by the fact that the filling approximation has been employed in the calculations for the $^{28}\text{Si} + ^{28}\text{Si}$ system. One such consideration is the fact that the Q value of the reaction is considerably affected by the filling approximation. Thus, while the total binding energy of the separated ^{16}O and ^{40}Ca ions, as computed using the local Skyrme interaction, is 442 MeV, 28 MeV less than the experimental value, the total binding energy of the separated ^{28}Si ions is but 370 MeV, 103 MeV less than the experimental value. The 75 MeV discrepancy in binding energy of the two systems can be used to explain, at least in a qualitative sense, the reason why the low angular momentum cutoff occurs at a much lower energy in the $^{28}\text{Si} + ^{28}\text{Si}$ system than in the $^{16}\text{O} + ^{40}\text{Ca}$ system. Other effects must be considered as well. Thus, for the $^{16}\text{O} + ^{40}\text{Ca}$ system, $\frac{1}{4}(16 + 40) = 14$ orbitals are involved in the calculation, while for the $^{28}\text{Si} + ^{28}\text{Si}$ system, because of the filling approximation, $\frac{1}{4}(40 + 40) = 20$ orbitals are involved in the calculation. The intent of this discussion is to emphasize that no clear cut statement as to the importance of entrance channel effects is possible on the basis of the present calculations.

IV. SUMMARY

We have calculated fusion cross sections for the systems $^{16}\text{O} + ^{40}\text{Ca}$ and $^{28}\text{Si} + ^{28}\text{Si}$, both of which lead to the compound system ^{56}Ni . Both systems exhibit an angular momentum window for fusion. The $^{16}\text{O} + ^{40}\text{Ca}$ results are in reasonable agreement with experiment,²⁴ and the $^{28}\text{Si} + ^{28}\text{Si}$ results are consistent with the experimental data²⁵ on the similar $^{32}\text{S} + ^{27}\text{Al}$ system.

The fusion results are qualitatively similar for the $^{16}\text{O} + ^{40}\text{Ca}$ and $^{28}\text{Si} + ^{28}\text{Si}$ systems, but do display

significant quantitative differences.²⁶ Thus, the $^{16}\text{O} + ^{40}\text{Ca}$ system can fuse with an angular momentum $l = 62$, while the maximum angular momentum with which the $^{28}\text{Si} + ^{28}\text{Si}$ system is calculated to fuse is $l = 50$. For comparison, the limiting angular momentum which the $A = 56$ system can sustain is given by the liquid drop model as $l = 58$.

The results calculated using the two-dimensional separable approximation are in very good agreement with the results of the fully three-dimensional calculations, except in the case of the most energetic of the $^{28}\text{Si} + ^{28}\text{Si}$ reactions. The rotating frame approximation, as in past calculations is accurate just above the Coulomb barrier, but breaks down for energies greater than that at which a fusion window develops. The effect of removing the neutron-proton degeneracy increases the $^{16}\text{O} + ^{40}\text{Ca}$ fusion cross section by approximately 120 mb over the energy range studied. The effect of the nonlocal terms in the Skyrme interaction is not clear at the single energy at which comparison was attempted. The difference in fusion cross section, as computed using the full Skyrme and local Skyrme interactions is not inconsistent with the difference which could be attributed to the fact that the full Skyrme calculation does not enforce isospin symmetry.

Perhaps the most striking result of the TDHF calculations remains the prediction of an angular momentum window for fusion. While both the $^{16}\text{O} + ^{40}\text{Ca}$ and $^{28}\text{Si} + ^{28}\text{Si}$ results are consistent with experiment, it would be exciting if a definitive experiment could determine whether such a window indeed does exist.

ACKNOWLEDGMENTS

This research was supported in part by the National Science Foundation [PHY77-21602, PHY76-83685, NSF77-12879], by the Division of Physical Research, U.S. Department of Energy, under Contract No. W-7405-eng-26 with the Union Carbide Corporation, and by the Lawrence Livermore Laboratory, U.S. Department of Energy, under Contract No. W-7405-eng-48. S. E. Koonin acknowledges the support of the Alfred P. Sloan Foundation.

¹P. A. M. Dirac, Proc. Cambridge Philos. Soc. 26, 376 (1930).

²P. Bonche, S. Koonin, and J. W. Negele, Phys. Rev. C 13, 1226 (1976).

³P. Bonche, J. Phys. (Paris) 37 Colloq. C5, 213 (1976).

⁴S. Koonin, Phys. Lett. 61B, 227 (1976).

⁵S. E. Koonin, K. T. R. Davies, V. Maruhn-Rezwani, H. Feldmeier, S. J. Krieger, and J. W. Negele, Phys.

Rev. C 15, 1359 (1977).

⁶V. Maruhn-Rezwani, K. T. R. Davies, and S. E. Koonin, Phys. Lett. 67B, 134 (1977).

⁷R. Y. Cusson and J. Maruhn, Phys. Lett. 62B, 134 (1976).

⁸J. A. Maruhn and R. Y. Cusson, Nucl. Phys. A270, 437 (1976).

⁹J. W. Negele, S. E. Koonin, P. Moller, J. R. Nix, and

- A. J. Sterk, Phys. Rev. C 17, 1098 (1978).
- ¹⁰K. T. R. Davies, V. Maruhn-Rezwani, S. E. Koonin, and J. W. Negele, Phys. Rev. Lett. 41, 632 (1978).
- ¹¹S. J. Krieger and K. T. R. Davies, Phys. Rev. C 18, 2567 (1978).
- ¹²K. R. Sandhya Devi and M. R. Strayer, J. Phys. G 4, L97 (1978); Phys. Lett. 77B, 135 (1978).
- ¹³K. T. R. Davies, H. T. Feldmeier, H. Flocard, and M. S. Weiss, Phys. Rev. C 18, 2631 (1978).
- ¹⁴S. E. Koonin, B. Flanders, H. Flocard, and M. S. Weiss, Phys. Lett. 77B, 13 (1978).
- ¹⁵R. Y. Cusson, R. K. Smith, and J. Maruhn, Phys. Rev. Lett. 36, 1166 (1976).
- ¹⁶R. Y. Cusson, J. A. Maruhn, and H. W. Meldner, Phys. Rev. C 18, 2589 (1978).
- ¹⁷H. Flocard, S. E. Koonin, and M. S. Weiss, Phys. Rev. C 17, 1682 (1978).
- ¹⁸P. Bonche, B. Grammaticos, and S. E. Koonin, Phys. Rev. C 17, 1700 (1978).
- ¹⁹T. H. R. Skyrme, Philos. Mag. 1, 1043 (1956); Nucl. Phys. 9, 615 (1959).
- ²⁰S. Cohen, F. Plasil, and W. J. Swiatecki, Ann. Phys. (N.Y.) 82, 557 (1974).
- ²¹While the actual value of l_c does depend upon the symmetries imposed upon the TDHF wave function, it is likely that the limit would remain in a totally unrestricted TDHF calculation. Although it is true that the removal of enforced symmetries, such as axial symmetry, and neutron-proton degeneracy, can enlarge the fusion window, our experience suggests that the limit will remain in a purely mean field calculation.
- ²²Referring to Fig. 15 of Ref. 20, we note that for values of $l \geq 42$, the fission barrier for $A = 56$ is calculated to be less than 8 MeV. Thus, on the basis of the liquid drop model, the $A = 56$ system is expected to fission for angular momenta $42 < l < 58$.
- ²³D. G. Kovar (unpublished); F. Plasil (unpublished).
- ²⁴S. E. Vigdor, D. G. Kovar, P. Speer, J. Mahoney, A. Menchaca-Rocha, C. Olmer, and M. S. Zisman (unpublished).
- ²⁵J. B. Natowitz, G. Doukellis, B. Kolb, G. Rosner, and Th. Walcher (unpublished).
- ²⁶It should be iterated that the initial ^{28}Si wave functions are not pure HF wave functions, but are calculated in the filling approximation. Thus, as discussed at the conclusion of Sec. III, no clear cut conclusion can be drawn as to the importance of entrance channel effects.
- ²⁷The dynamical inhibition of fusion at low impact parameters has also been observed in Ca+Ca calculations based on the excitation of damped surface modes (Ref. 28), and in other macrophysics studies (Ref. 29).
- ²⁸R. A. Broglia, C. H. Dasso, G. Pollarolo, and A. Winther, Phys. Rev. Lett. 40, 707 (1978).
- ²⁹C. F. Tsang, Phys. Scr. 10A, 90 (1974); K. Siwek-Wilczynska and J. Wilczynski, Nucl. Phys. A264, 115 (1976).
- ³⁰In the separable approximation, the required orthogonality of the orbitals (as a function of the coordinate perpendicular to the reaction plane) demands that the same harmonic oscillator parameter be used for both the ^{16}O ion and the ^{40}Ca ion. In the present calculation, the parameter employed is the mean of that appropriate to the individual ions. Since the latter parameters differ by but 10%, the effect upon the calculation is negligible. This point will be fully discussed in the forthcoming publication by B. Flanders, P. Bonche, S. E. Koonin, and M. S. Weiss.